

Lowest Energy Excited States of Unsaturated Cyclic  $M_3(dppm)_3CO^{2+}$  Clusters ( $M = Pd, Pt$ )

Pierre D. Harvey\* and Réjean Provencher

Département de chimie, Université de Sherbrooke, Sherbrooke, Québec, Canada J1K 2R1

Received May 27, 1992

The nature of the lowest energy excited states of cyclic unsaturated  $M_3(dppm)_3CO^{2+}$  clusters ( $M = Pd, Pt$ ) has been addressed experimentally using UV–visible, emission, and polarized excitation emission spectroscopy, emission lifetime measurements, and EHMO computations. The 77 K UV–visible spectra exhibit low-intensity features [at 570 nm ( $\epsilon = 1500 \text{ M}^{-1} \text{ cm}^{-1}$ ;  $M = Pd$ ) and at 460 nm ( $\epsilon = 3200 \text{ M}^{-1} \text{ cm}^{-1}$ ;  $M = Pt$ )]; they are assigned to singlet–triplet absorptions ( $^3A_2, ^3E \leftarrow ^1A_1$ ) on the basis of comparison of the Stokes shifts and  $\epsilon$  values with those for the  $M_2(dppm)_3$  complexes ( $M = Pd, Pt$ ). The more intense features located at 483 nm ( $\epsilon = 43\,400 \text{ M}^{-1} \text{ cm}^{-1}$ ) and 413 nm ( $\epsilon = 10\,900 \text{ M}^{-1} \text{ cm}^{-1}$ ) for  $M = Pd$  and  $Pt$ , respectively, are assigned to the  $^1E \leftarrow ^1A_1$  ( $a_2 \leftarrow e$ ) transitions. The unobserved and forbidden  $a_2 \leftarrow a_1$  electronic transitions give rise to the  $^1,^3A_2$  excited states. It was not possible to definitely assign the lowest energy triplet excited states ( $^3A_2$  or  $^3E$ ) on the basis of polarization measurements, but we find that these states must lie nearby in energy (within a few hundred wavenumbers). The clusters are luminescent at low temperatures ( $\lambda_{\text{max}} = 705$ ,  $M = Pd$ ;  $\lambda_{\text{max}} = 620$  nm,  $M = Pt$ ) where the emission lifetimes,  $\tau_e$  (77 K), are  $2.4 \pm 0.1$  and  $14.0 \pm 0.4 \mu\text{s}$  (in 2-MeTHF and in PrCN), and  $3.83 \pm 0.04$  and  $3.73 \pm 0.05 \mu\text{s}$  (solid state), for  $M = Pd$  and  $Pt$ , respectively. The quantum yields,  $\Phi_e$  (77 K) are  $<0.001$  and  $\sim 0.013$  for  $M = Pd$  and  $Pt$ , respectively, in 2-MeTHF solutions. No luminescence is observed at room temperature, and the excited lifetimes, measured from flash photolysis measurements, are  $80 \pm 10$  ps and  $80 \pm 10$  ns for  $M = Pd$  and  $Pt$ , respectively.

## Introduction

The coordinatively unsaturated cyclic  $M_3(dppm)_3CO^{2+}$  clusters ( $M = Pd, Pt$ ;  $dppm = ((C_6H_5)_2P)_2CH_2$ ) represent an interesting family of compounds that exhibit rich addition and oxidative addition reactivities.<sup>1,2</sup> Of particular interest, the  $Pt_3(dppm)_3CO^{2+}$  cluster has been found to be a catalyst for the water gas shift reaction,<sup>3</sup> to be a good model for substrate–surface binding interactions between the acetylene molecule and  $Pt(111)$ ,<sup>4</sup> and, more recently, to be a model for mercury–platinum amalgams.<sup>5</sup> The main structural features in these clusters are that the complexes exhibit three unsaturated metal atoms that are encircled by a cylindrical array of phenyl rings (“picket-fence-like”) which is essentially a small triangular metal surface situated in a hydrophobic cavity.<sup>6a,b</sup> Examples of coordinatively unsaturated clusters of this type (“ $M_3(dppm)_3$ ”)<sup>6c</sup> are rare, as compared to the bicapped compounds that are reported in the literature<sup>2,4,5,7</sup> and also to the closely-related 42-electron trinuclear clusters ( $D_{3h}$

symmetry)  $M_3L_3(\mu-L')_3$  ( $M = Pd, Pt$ ;  $L =$  phosphines and isocyanides;  $L' = CO, SO_2, CS_2$ , and isocyanides).<sup>8</sup> Despite the low occurrence of the monocapped  $M_3$  complexes,<sup>1,6</sup> these clusters have attracted some attention from a theoretical (EHMO) viewpoint.<sup>9</sup>

The  $M_3(dppm)_3CO^{2+}$  clusters ( $M = Pd, Pt$ ) are found to be luminescent at 77 K (which is not uncommon for low-valent  $Pd$  and  $Pt$  mono- and polynuclear complexes)<sup>10</sup> and exhibit interesting photoinduced activation of C–H bonds and of small molecules ( $CO, CO_2, H_2$ , and  $O_2$ ).<sup>11</sup> To our knowledge, there have been no experimental investigations of the accessible low-energy excited electronic states, of the electronic structures or of the MO schemes of the monocapped  $M_3(dppm)_3CO^{2+}$  clusters ( $M = Pd, Pt$ ). However, a single spectroscopic study on a structurally related complex,  $Pt_3(\mu-CO)_3(P(t-Bu)_3)_3$ , has addressed the nature of the frontier orbitals in some detail.<sup>12</sup> In order to assign and characterize the nature of the lowest energy excited state, we now wish to report their 77 K UV–vis spectra, along with EHMO computations (for both  $Pd$  and  $Pt$  clusters for comparison purposes), their 77 K emission spectra and polarization ratio of

- (1) (a) Ferguson, G.; Lloyd, B. F.; Manojlovic-Muir, L.; Muir, K. W.; Puddephatt, R. J. *Inorg. Chem.* **1986**, *25*, 4190. (b) Jennings, M. C.; Puddephatt, R. J. *Inorg. Chem.* **1988**, *27*, 4280. (c) Lloyd, B. R.; Bradford, A.; Puddephatt, R. J. *Organometallics* **1987**, *6*, 424. (d) Douglas, G.; Jennings, M. C.; Manojlovic-Muir, L.; Muir, K. W.; Puddephatt, R. J. *J. Chem. Soc., Chem. Commun.* **1989**, 159. (e) Bradford, A. M.; Jennings, M. C.; Puddephatt, R. J. *Organometallics* **1989**, *8*, 2367.
- (2) Manojlovic-Muir, L.; Muir, K. W.; Lloyd, B. R.; Puddephatt, R. J. *J. Chem. Soc., Chem. Commun.* **1985**, 536.
- (3) Puddephatt, R. J. *Can. Chem. New* **1986**, *38*, 6.
- (4) (a) Rashidi, M.; Puddephatt, R. J. *J. Am. Chem. Soc.* **1986**, *108*, 7111. (b) Douglas, G.; Manojlovic-Muir, L.; Muir, K. W.; Rashidi, M.; Anderson, C. M.; Puddephatt, R. J. *J. Am. Chem. Soc.* **1987**, *109*, 6527. (c) Rashidi, M.; Puddephatt, R. J. *Organometallics* **1988**, *7*, 1636.
- (5) Schoettel, G.; Vittal, J. J.; Puddephatt, R. J. *J. Am. Chem. Soc.* **1990**, *112*, 6400.
- (6) (a) Ferguson, G.; Lloyd, B. R.; Puddephatt, R. J. *Organometallics* **1986**, *5*, 344. (b) Manojlovic-Muir, L.; Muir, K. W.; Lloyd, B. R.; Puddephatt, R. J. *J. Chem. Soc., Chem. Commun.* **1983**, 1336. (c) See for example: Ho, D. M.; Bau, R. *Inorg. Chem.* **1983**, *22*, 4079.
- (7) (a) Aly, A. A. M.; Neugebauer, D.; Orama, O.; Schubert, U.; Schmidbauer, H. *Angew. Chem., Int. Ed. Engl.* **1978**, *17*, 125. (b) Schubert, U.; Neugebauer, D.; Aly, A. A. M. *Z. Anorg. Allg. Chem.* **1980**, *464*, 217. (c) Bresciani, N.; Marsich, N.; Nardin, G.; Randaccio, L. *Inorg. Chim. Acta* **1974**, *10*, L5. (d) Nardin, G.; Randaccio, L.; Zangrando, E. *J. Chem. Soc., Dalton Trans.* **1975**, 2566. (e) Camus, A.; Marsich, N.; Nardin, G.; Randaccio, L. *J. Organomet. Chem.* **1973**, *60*, C39. (f) Ratliff, K. S.; Fanwick, P. E.; Kubiak, C. *Polyhedron* **1990**, *9*, 1387.

- (8) (a) For a review, see: Mingos, D. M. P.; Wardle, R. W. M. *Transition Met. Chem. (London)* **1985**, *10*, 441. (b) Albinati, A. *Inorg. Chim. Acta* **1977**, *22*, L31. (c) Goel, R. G.; Ogin, W. O.; Srivastava, R. C. *J. Organomet. Chem.* **1981**, *214*, 405. (d) Evans, D. G.; Hallam, M. F.; Mingos, D. M. P.; Wardle, R. W. M. *J. Chem. Soc., Dalton Trans.* **1987**, 1889. (e) Green, M.; Howard, J. A. K.; Murray, M.; Spencer, J. L.; Stone, F. G. A. *J. Chem. Soc., Dalton Trans.* **1977**, 1509. (f) Moody, D. C.; Ryan, R. R. *Inorg. Chem.* **1977**, *16*, 1052. (g) Ritchey, J. M.; Moody, D. C. *Inorg. Chim. Acta* **1983**, *72*, 271. (h) Ritchey, J. M.; Moody, D. C.; Ryan, R. R. *Inorg. Chem.* **1983**, *22*, 2276.
- (9) (a) Mealli, C. *J. Am. Chem. Soc.* **1985**, *107*, 2245. (b) Evans, D. G. *J. Organomet. Chem.* **1988**, *352*, 397.
- (10) (a) Harvey, P. D.; Schaefer, W. P.; Gray, H. B. *Inorg. Chem.* **1988**, *27*, 1101. (b) Harvey, P. D.; Gray, H. B. *J. Am. Chem. Soc.* **1988**, *110*, 2145. (c) Harvey, P. D.; Adar, F.; Gray, H. B. *J. Am. Chem. Soc.* **1989**, *111*, 1312. (d) Harvey, P. D.; Gray, H. G. *Polyhedron* **1990**, *9*, 1949. (e) Harvey, P. D.; Gan, L. *Inorg. Chem.* **1991**, *30*, 3239. (f) Caspar, J. V. *J. Am. Chem. Soc.* **1985**, *107*, 6718. (g) Kane-Maguire, N. A. P.; Wright, L. L.; Guckert, J. A.; Tweet, W. S. *Inorg. Chem.* **1988**, *27*, 2905. (h) Baralt, E.; Boudreaux, E. A.; Demas, J. N.; Lenhart, P. G.; Lukehart, C. M.; McPhail, A. T.; McPhail, D. R.; Myers, J. B., Jr.; Saksater, L.; True, W. R. *Organometallics* **1989**, *8*, 2417.
- (11) Harvey, P. D.; Socol, S. Unpublished results.
- (12) Jaw, H.-R. C.; Mason, W. R. *Inorg. Chem.* **1990**, *29*, 3452.

the excitation spectra, and their excited-state lifetimes. The spectra are partially interpreted with the use of EHMO computations.<sup>9</sup>

## Experimental Section

**Materials.** The  $M_3(\text{dppm})_3\text{CO}_2^{2+}$  clusters ( $M = \text{Pd}, \text{Pt}$ ; counteranions =  $\text{PF}_6^-$ ,  $\text{CF}_3\text{CO}_2^-$ ) were synthesized according to published procedures.<sup>1</sup> All solvents used, namely, acetonitrile (BDH), methanol (BDH), acetone (Fisher Scientific Co.), dimethoxyethane (Fisher Scientific Co.), dimethylformamide (BDH), tetrahydrofuran (Aldrich Chemical Co.), toluene (Mallinckrodt), 2-propanol (BDH), ethanol (100% BDH), dichloromethane (Mallinckrodt), butyronitrile (Aldrich Chemical Co.), and 2-methyltetrahydrofuran (Aldrich Chemical Co.), were purified according to standard procedures.<sup>13</sup>

**Spectroscopic Measurements.** The absorption spectra were measured on a Hewlett Packard 8452A diode array spectrophotometer. The 77 K spectra were acquired using a homemade Dewar assembly where the cell was 0.5 cm thick. Typical concentration were  $(3-6) \times 10^{-5}$  M. The 77 K absorptivity measurements were corrected for glass contraction. The corrected emission, excitation, and polarized spectra were obtained using a Spex Fluorolog II spectrometer or the steady-state LS100 system from Photon Technology Inc. The emission lifetimes were measured using an LS100 phosphorimeter system (Photon Technology Inc.) fitted with a tungsten EG & G Model FX-280 microsecond flash-lamp source ( $\sim 1$   $\mu\text{s}$  fwhm).

**Experimental Procedures.** The polarization ratios ( $N$ ) of the excitation emission spectra were measured using procedures outlined by Johnson.<sup>14</sup> To ensure that our setup was correct, we have also reproduced the data on carbazole reported by Johnson.<sup>14</sup> The emission quantum yields,  $\Phi_e$ , were obtained using 9,10-diphenylanthracene as the standard [ $\Phi_e = 1.0$  (77 K)].<sup>15</sup> All solutions were freeze-pump-thaw degassed prior to measurements and kept in the dark (since the complexes are slightly light sensitive in the presence of oxygen).

**Flash Photolysis Measurements.** The 298 K excited-state lifetimes of the  $M_3(\text{dppm})_3\text{CO}_2^{2+}$  clusters ( $M = \text{Pd}, \text{Pt}$ ) were measured from the recovery of ground-state bleaching in flash photolysis experiments that were performed at the Center for Fast Kinetics (Austin, TX). These picosecond time-resolved measurements were performed in the following way: the laser source for the picosecond time-resolved kinetic measurements was a mode-locked Nd:YAG laser (Quantel YG 402). Both the harmonic (532 or 355 nm) and the residual (1064 nm) light pulses were extracted from the laser and traveled together to a dichroic mirror that reflected the harmonic laser pulse in a 90° angle and transmitted the 1064-nm light. While the harmonic light was focused onto the sample cuvette, the 1064-nm light traversed a variable delay stage before being focused onto a 10-cm cuvette containing a 50:50 mixture of deuteriated phosphoric acid and  $\text{D}_2\text{O}$  to produce a white continuum light flash of 30-ps duration. The continuum light was focused through a diffusing frosted glass plate, recollimated, and focused onto the common end of a bifurcated fiber optics bundle that split the beam into two branches, a sample beam that probed the sample where it was excited by the harmonic laser pulse (excited state) and a reference beam that probed the sample where it was not excited (ground state). The two light beams were picked up by fiber optics on the other side of the cuvette and led to a UFS 200 spectrograph to which a dual diode array ( $2 \times 512$ ) with image intensifier was attached. Thus, with one single continuum flash, the spectra of excited and unexcited samples could be detected. The wavelength resolution of the system was 1 nm per diode. The diode array data were passed via a Tracor Northern 6200 multichannel analyzer to a personal computer for storage, analysis, and display. In a typical experiment, about 200 spectra were averaged for one delay time. By moving the delay stage, the arrival of the continuum flash could be delayed by up to 5 ns with respect to the excitation pulse, thus generating time-resolved spectra with a time resolution limited only by the pulse width of the laser (ca. 30 ps). Before each measurement, the two diode arrays were balanced for all reference absorption of the transient species for each wavelength:  $A = \log(I(\text{reference})/I(\text{sample}))$ .

- (13) (a) Perrin, D. D.; Armarego, W. L. F.; *Purification of Laboratory Chemicals*, 3rd ed.; Pergamon: Oxford, U.K., 1988. (b) Gordon, A. J.; Ford, R. A. *The Chemist's Companion. A Handbook of Practical Data, Techniques, and References*; Wiley: New York, 1972.  
 (14) Johnson, G. E. *J. Chem. Phys.* 1974, 78, 1512.  
 (15) Lim, E. C.; Lapos, J. D.; Yu, J. M. H. *J. Mol. Spectrosc.* 1966, 19, 412.

**Table I.** Comparison of the Spectroscopic 298 K Data for  $\text{Pd}_3(\text{dppm})_3\text{CO}_2^{2+}$

solvent	$\text{CF}_3\text{COO}^-$			$\text{PF}_6^-$		
	$\lambda_{\text{max}}$ (nm)	$\nu_{\text{max}}$ ( $\text{cm}^{-1}$ )	$\epsilon$ ( $\text{M}^{-1} \text{cm}^{-1}$ )	$\lambda_{\text{max}}$ (nm)	$\nu_{\text{max}}$ ( $\text{cm}^{-1}$ )	$\epsilon$ ( $\text{M}^{-1} \text{cm}^{-1}$ )
acetonitrile	476	21 000	21 200	474	21 100	22 500
MeOH	494	20 200	23 500	492	20 300	23 200
toluene	488	20 500	29 800	484	20 700	31 100
<i>i</i> -PrOH	484	20 700	27 400	484	20 700	20 700
$(\text{CH}_3\text{OCH}_2)_2$	488	20 500	24 700	482	20 700	16 600
acetone	488	20 500	26 610	484	20 700	24 800
$\text{CH}_2\text{Cl}_2$	484	20 700	28 800	484	20 700	29 000
EtOH	480	20 800	27 500	482	20 700	27 500
THF	488	20 500	29 000	486	20 600	27 900
DMF	466	21 500	26 000	464	21 600	25 400

**Computational Details.** All of the MO calculations were of the extended Hückel type (EHMO)<sup>16</sup> using a modified version of the Wolfsberg-Helmholz formula.<sup>17</sup> The atomic parameters used for C,<sup>16</sup> O,<sup>16</sup> P,<sup>18a</sup> H,<sup>16</sup> Pd,<sup>18b</sup> and Pt<sup>18a</sup> were from the literature. The  $M_3(\text{dppm})_3\text{CO}_2^{2+}$  crystal structure data that were used<sup>6a,b</sup> had Pd-Pd, Pt-Pt, Pd-C, Pt-C, Pd-P, Pt-P, and P-H<sup>19</sup> distances fixed at 2.60, 2.63, 2.13, 2.09, 2.30, 2.30, and 1.05 Å, respectively. The detailed description for the graphic programs used in this work can be found in ref 20.

## Results and Discussion

**1. UV-Visible Spectra and EHMO Computations.** The 298 K UV-visible spectra (350–550 nm) for  $M_3(\text{dppm})_3\text{CO}_2^{2+}$  clusters are characterized by structureless bands located at  $\sim 484$  nm ( $M = \text{Pd}$ ) and 380 nm ( $M = \text{Pt}$ ). Both band shapes and adsorptivities ( $\epsilon$ ) for the bands are found to be sensitive to the solvent media and the various substrates that could be present in solution (see Table I for details in the case of  $\text{Pd}_3(\text{dppm})_3\text{CO}_2^{2+}$ ). Such behavior has previously been reported for  $\text{Pd}_3(\text{dppm})_3\text{CO}_2^{2+}$  with halide and  $\text{CF}_3\text{CO}_2^-$  anions in methanol solution.<sup>2</sup> In the latter case, it was crystallographically shown that the various electron-donor substrates were coordinatively added to the unsaturated sites of the Pd cluster within the cavity and that this process was accompanied by spectroscopic changes.<sup>2</sup> In this work, a similar behavior is observed, where isosbestic points appear in the spectra upon addition of a different solvent to the solutions. In the  $\text{Pt}_3(\text{dppm})_3\text{CO}_2^{2+}$  case, the  $\lambda_{\text{max}}$  and  $\epsilon$  values only vary between 380 and 382 nm and between 15 200 and 16 800  $\text{M}^{-1} \text{cm}^{-1}$ , respectively (details available in the supplementary material). In these cases, cluster-substrate interactions are less pronounced. No equilibrium constants are measured, but changes in photophysical properties are anticipated, dependent upon the nature of the substrate that is present in the cavity.

The 77 K spectra (see Figure 1 for example) for both clusters in 2-MeTHF and PrCN reveal new features (spectroscopic data are listed in Table II). Of particular interest, low-intensity shoulders that are located at 570 nm ( $\epsilon = 1500$ ) and 460 nm ( $\epsilon = 3200 \text{ cm}^{-1} \text{ M}^{-1}$ ), for  $M = \text{Pd}$  and  $\text{Pt}$ , respectively (2-MeTHF data), are now observed. These bands exhibit some forbidden characters, and their adsorptivities are very similar to those found for singlet-triplet absorptions in the  $M_2(\text{dppm})_3$  complexes ( $M = \text{Pd}, \text{Pt}$ ;  $\epsilon(^3(p\sigma \leftarrow d\delta^*)) = 2500$  and 5100,  $\epsilon(^3(p\sigma \leftarrow d\sigma^*)) = 530$  and 1200  $\text{cm}^{-1} \text{ M}^{-1}$ , respectively).<sup>10b</sup> The Stokes shifts ( $\Delta$ )

- (16) (a) Hoffmann, R.; Lipscomb, W. M. *J. Chem. Phys.* 1962, 36, 2179. (b) Hoffmann, R.; Lipscomb, W. N. *J. Chem. Phys.* 1962, 37, 2872. (c) Hoffmann, R. *J. Chem. Phys.* 1963, 39, 1397.  
 (17) Ammeter, J. H.; Burgi, H. B.; Thibeault, J. C.; Hoffmann, R. *J. Am. Chem. Soc.* 1978, 100, 3686.  
 (18) (a) Summerville, R. H.; Hoffmann, R. *J. Am. Chem. Soc.* 1976, 98, 7240. (b) Tatsumi, K.; Hoffmann, R.; Yamamoto, A.; Stille, J. K. *Bull. Chem. Soc. Jpn.* 1981, 54, 1857.  
 (19) Because of limitations in the size of the molecules handled by the program, each dppm ligand was replaced by two  $\text{PH}_3$  ligands. Hence the computed molecules are  $M_3(\text{PH}_3)_6\text{CO}_2^{2+}$  ( $M = \text{Pd}, \text{Pt}$ ). This methodology is a standard one.<sup>9b</sup>  
 (20) Mealli, C.; Proserpio, D. M. *J. Chem. Educ.* 1990, 67, 399.

Table II. 77 K Spectroscopic Data<sup>a</sup>

$Pd_3(dppm)_3CO^{2+}$						$Pt_3(dppm)_3CO^{2+}$					
2-MeTHF			PrCN			2-MeTHF			PrCN		
$\lambda$ (nm)	$\bar{\nu}$ (cm <sup>-1</sup> )	$\epsilon$ (M <sup>-1</sup> cm <sup>-1</sup> )	$\lambda$ (nm)	$\bar{\nu}$ (cm <sup>-1</sup> )	$\epsilon$ (M <sup>-1</sup> cm <sup>-1</sup> )	$\lambda$ (max)	$\bar{\nu}$ (cm <sup>-1</sup> )	$\epsilon$ (M <sup>-1</sup> cm <sup>-1</sup> )	$\lambda$ (max)	$\bar{\nu}$ (cm <sup>-1</sup> )	$\epsilon$ (M <sup>-1</sup> cm <sup>-1</sup> )
570	17 500	1 500	581	17 200	2 500	461	21 700	3 200	463	21 600	3 600
483	20 700	43 400	489	20 500	42 700	413	24 200	10 900	417	24 000	9 800
457	21 900	37 600	465	21 500	39 200	382	26 200	20 600	386	25 900	17 800
370	27 000	8 900	373	26 800	5 500	362	27 600	17 400	360	27 800	14 800
						327	30 600	24 200	321	31 200	26 200
311	32 100	64 700	324	30 900	51 900	288	34 700	48 500	293	34 100	43 700

<sup>a</sup> The  $\bar{\nu}$  values do not change with the counteranions. The  $\epsilon$  measurements were performed for the  $CF_3CO_2^-$  salt for  $M = Pd$  and for the  $PF_6^-$  salt for  $M = Pt$ .

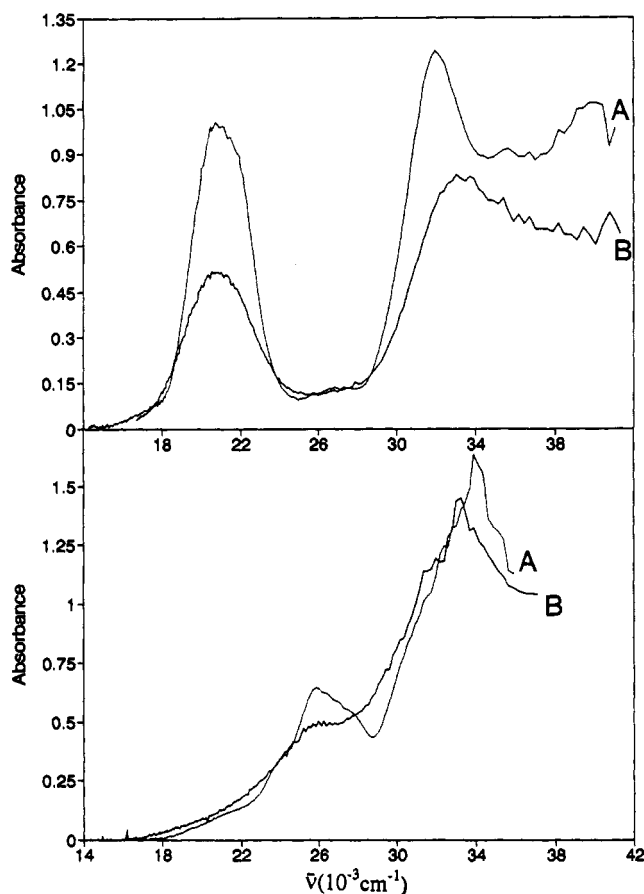


Figure 1. Comparison of the electronic spectra of  $M_3(dppm)_3CO^{2+}$  clusters ( $M = Pd$ , top;  $M = Pt$ , bottom) at 77 K (A) and 298 K (B) in butyronitrile. The spectra at 77 K were not corrected for glass contraction; the spectra were obtained from the same solutions that were prepared at 298 K.

found in  $M_3(dppm)_3CO^{2+}$  are 3300 and 4600  $cm^{-1}$  for  $M = Pd$  and  $Pt$ , respectively, and are common values for low-valent polynuclear  $Pd$  and  $Pt$  complexes.<sup>10b,c</sup> As examples, the  $\Delta$  values found for the  $M_2(dppm)_3$  complexes are 3000 and 4200  $cm^{-1}$  for  $M = Pd$  and  $Pt$  respectively, and for the  $M_2(dba)_3$  compounds are 5100 and 4800  $cm^{-1}$  for  $M = Pd$  and  $Pt$ , respectively.<sup>1b,c</sup> We assign these weak features to singlet-triplet absorptions ( $^3A_2$ ,  $^3E \leftarrow ^1A_1$ ; see text below). Due to the relatively large number of excited states that are close in energy (presumably within a few hundred wavenumbers), it is not possible to make any specific assignments, and these features must be considered as a convolution of more than one single-triplet absorption. The electronic spectra of the clusters are sensitively different in band positions and absorptivities. This phenomenon can be explained, in part, using the comparison of the qualitative EHMO computations for  $Pd$  and  $Pt$ .

The EHMO analysis for  $Pt_3(dppm)_3CO^{2+}$  has been reported,<sup>9</sup> but, unfortunately, not the relative MO energies. We have

Table III. Comparison between the Computed Energies for Selected Cluster Molecular Orbitals and Electronic Transitions<sup>a</sup>

MO	polarizn	$Pd_3(dppm)_3CO^{2+}$	$Pt_3(dppm)_3CO^{2+}$
$a_1 \rightarrow a_2^b$		1.005 (8106)	1.885 (15 200)
$e(36,37) \rightarrow a_2$	$x,y$	1.533 (12 360)	2.393 (19 300)
$e(38,39) \rightarrow a_2$	$x,y$	1.692 (13 650)	2.553 (20 600)
$a_1 \rightarrow e$	$x,y$	2.199 (17 740)	3.117 (25 140)
$e \rightarrow e$	$z$	2.727 (22 000)	3.277 (26 430)

<sup>a</sup> Units: eV; values in parentheses are in  $cm^{-1}$ . <sup>b</sup> Orbitaly forbidden transition.

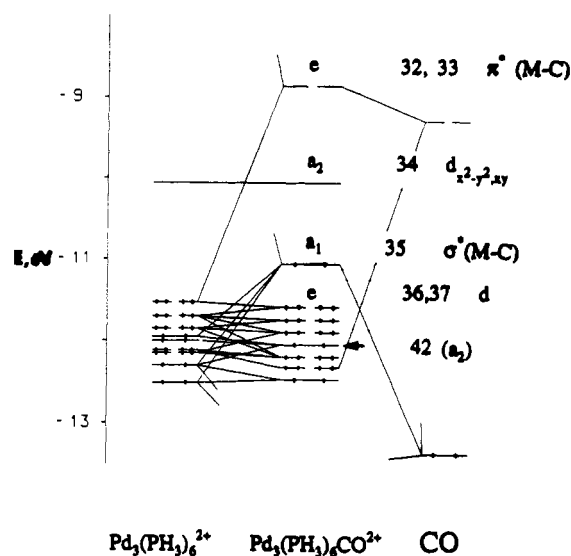
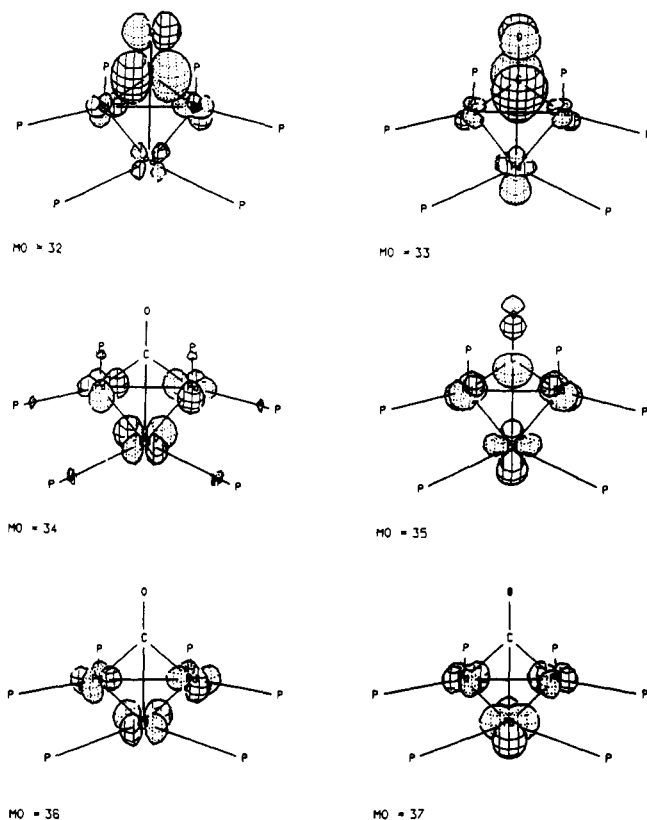


Figure 2. Fragment molecular diagram for  $Pd_3(PH_3)_6CO^{2+}$  ( $C_{3v}$  point group) showing the MO numbering used in this work. The arrow refers to orbital 42 ( $a_2$ ), which is discussed in the text.

recomputed EHMO energies for  $Pt_3(dppm)_3CO^{2+}$  and compared them with ours for  $Pd_3(dppm)_3CO^{2+}$  (Table III). The MO analyses (Figure 2) for both clusters are essentially identical and agree with the literature.<sup>9</sup> From data listed in Table III, one can easily depict the relative energy gaps between MO's corresponding to the lowest energy electronic transitions (Table III). The data clearly show that each electronic transition for the  $Pd$  compound is systematically red-shifted with respect to the  $Pt$  cluster (which is in agreement with the UV-visible spectroscopic observations). The absorptivity difference between the spectra depends upon a number of factors, which cannot be accurately addressed with the type of computations used in this work.

A picture of MO's 32, 33 ( $e$ ), 34 ( $a_2$ ; LUMO), 35 ( $a_1$ , HOMO), and 36, 37 ( $e$ ) is provided in Figure 3. The computed EHMO atomic contributions for these orbitals are provided in the supplementary material. The 32, 33 ( $e$ ) orbitals are largely composed of  $\pi^*(CO)$  and metal  $d$  and  $p$  orbitals and are the antibonding  $\pi(M-C)^*$  molecular orbitals. The atomic contributions for the  $M_3$  framework are largely composed of  $p_z$  and  $d_{z^2}$  orbitals, and minor  $d_{xy}$ ,  $d_{yz}$ ,  $d_{xz}$ , and  $d_{x^2-y^2}$  components are also generated by the computations, in order to induce the appropriate



**Figure 3.** Visualization of selected MO's for  $\text{Pd}_3(\text{PH}_3)_6\text{CO}^{2+}$  (32, 33 = e; 34 =  $a_2$ ; 35 =  $a_1$ ; 36, 37 = e).

overlap between the metal and CO orbitals. The LUMO<sup>21</sup> is strictly composed of metal in-plane d orbitals ( $d_{xy}$ ,  $d_{x^2-y^2}$  with some minor  $p_x$ ,  $p_y$  contributions) and some phosphorus p components, ( $p_y$ ,  $p_x$ ), forming metal-metal and metal-phosphorus antibonding molecular orbitals. The HOMO (mostly metal d orbitals with some  $p_z$  and some C=O  $n$  and  $\sigma$  characters) is somewhat weakly metal-metal bonding in the plane and is metal-carbonyl antibonding. The M-M atomic interactions are very complex in this case, where contributions of practically all d and p metal orbitals are computed. MO's 36 and 37 originate strictly from the in-plane metal d and p orbitals and are metal-metal bonding. The MO diagram (Figure 2) shows that the LUMO is well "isolated" from the others and indicates that the two lowest energy electronic transitions are  $a_2 \leftarrow a_1$  and  $a_2 \leftarrow e$ . The former transition is forbidden by symmetry, while the latter is allowed and polarized in the metallic plane. The EHMO computations are qualitative ones, and an assignment of  $^3[1(a_2)^1(a_1)]^*$  as the lowest energy excited state needs to be experimentally demonstrated. Nevertheless, the observed low-energy and relatively intense bands for Pd (483 nm) and Pt (413 nm) are easily assigned to  $a_2 \leftarrow e$ .

**2. Emission Spectra and Lifetimes.** Upon cooling, the  $\text{M}_3(\text{dppm})_3\text{CO}^{2+}$  clusters (M = Pd, Pt) luminesce at temperatures approaching 77 K. Emission bands are observed at 705 nm (Pd) and 620 nm (Pt) and are relatively  $\lambda_{\text{max}}$  insensitive to the nature of the counteranions ( $\text{CF}_3\text{CO}_2^-$ ,  $\text{PF}_6^-$ ), both for the solid state and for solutions (Figure 4). On the other hand, both  $\tau_e$  and  $\Phi_e$  dramatically decrease between 77 K glasses and 298 K media. This behavior is very likely associated with the substrate-cluster interactions described earlier. This phenomenon is further confirmed by the  $\tau_e$  measurements for solid samples of

(21)  $\text{Pd}_3(\text{dppm})_3\text{CO}^{2+}$  undergoes a quasi-reversible 2-electron reduction at  $-0.70$  V vs SSCE (in a 1:1 DMF/acetonitrile mixture and 0.1 M LiCl supporting electrolyte) to form the neutral species  $\text{Pd}_3(\text{dppm})_3\text{CO}$ . The increase in  $\nu(\text{C}=\text{O})$  (from 1835 to 1967  $\text{cm}^{-1}$ ) during reduction suggests that the CO group now occupies a terminal position on one of the Pd atoms: Mugnier, Y.; Harvey, P. D. Unpublished results.

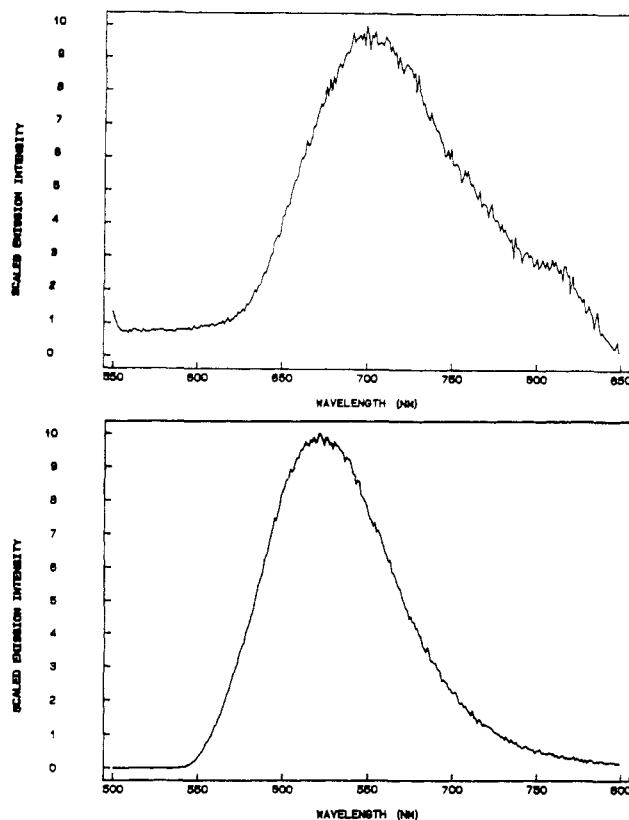


**Figure 4.** Corrected emission spectra of  $\text{M}_3(\text{dppm})_3\text{CO}^{2+}$  clusters (M = Pd (top), Pt (bottom)) in 2-MeTHF at 77 K. The shoulder located at 800 nm in the  $\text{Pd}_3(\text{dppm})_3\text{CO}^{2+}$  spectrum is an instrumental artifact.

**Table IV.** Triplet Excited-State Lifetimes of  $\text{M}_3(\text{dppm})_3\text{CO}^{2+}$  Compounds

medium	$\tau_e$	
	Pd (705 nm) <sup>a</sup>	Pt (620 nm) <sup>b</sup>
2-MeTHF (77 K)		$13.9 \pm 0.2 \mu\text{s}$
PrCN (77 K)	$2.4 \pm 0.1 \mu\text{s}$	$14.0 \pm 0.4 \mu\text{s}$
solid state (77 K)	$3.83 \pm 0.04 \mu\text{s}$	$3.73 \pm 0.05 \mu\text{s}$
toluene (298 K) <sup>c</sup>	$80 \pm 10 \text{ ps}$	$80 \pm 10 \text{ ns}$

<sup>a</sup> For the  $\text{CF}_3\text{CO}_2^-$  salt;  $\Phi_e < 0.001$ . <sup>b</sup> For the  $\text{PF}_6^-$  salt;  $\Phi_e = 0.013 \pm 0.001$  (2-MeTHF). <sup>c</sup> Measured from the recovery of transient bleaching by flash photolysis spectroscopy.

$[\text{Pd}_3(\text{dppm})_3\text{CO}](\text{CF}_3\text{CO}_2)_2$  and  $[\text{Pt}_3(\text{dppm})_3\text{CO}](\text{PF}_6)_2$  at 77 K, for which the X-ray structures have revealed the presence of one counteranion within the cluster cavity;<sup>6a,b</sup> the  $\tau_e$  values are smaller than that of the 77 K glass data (and are similar to each other). Usually the increased rigidity of a crystal should enhance  $\tau_e$  with respect to glasses (for all cases). In all of our measurements, decay and recovery were monoexponential. The long lifetimes and relatively large Stoke shifts (3300  $\text{cm}^{-1}$  for Pd and 4600  $\text{cm}^{-1}$  for Pt) indicate that these emissions are phosphorescent. No anomaly has been observed in the excitation spectra, since they correspond to absorption spectra.

We further notice that while the 77 and 293 K  $\tau_e$  data for  $\text{Pt}_3(\text{dppm})_3\text{CO}^{2+}$  compare very favorably with those for  $\text{Pt}_2(\text{dppm})_3$  ( $\tau_e \leq 20 \text{ ns}$  (at 293 K) and  $10.6 \pm 0.2 \mu\text{s}$  (at 77 K)),<sup>10b</sup> the  $\tau_e$  data for  $\text{Pd}_3(\text{dppm})_3\text{CO}^{2+}$  are unusually small. The  $\tau_e$  values reported for  $\text{Pd}_2(\text{dppm})_3$  are  $5.93 \pm 0.01 \mu\text{s}$  (at 293 K) and  $107 \pm 1 \mu\text{s}$  (at 77 K).<sup>10b</sup> These short  $\tau_e$  values are accompanied by a smaller  $\Phi_e$  value as well;  $\Phi_e(\text{Pd}_3(\text{dppm})_3\text{CO}^{2+}; 293 \text{ K}) < 0.001$  and  $\Phi_e(\text{Pd}_2(\text{dppm})_3; 293 \text{ K}) = 0.06$ .<sup>10f</sup> Typical spin-orbit coupling effects would generate shorter  $\tau_e$  values for the heavier elements; i.e.  $\tau_e(\text{Pd}) > \tau_e(\text{Pt})$ .<sup>10</sup> The unusually shorter  $\tau_e$  and  $\Phi_e$  values for  $\text{Pd}_3(\text{dppm})_3\text{CO}^{2+}$  in comparison with  $\text{Pt}_3(\text{dppm})_3\text{CO}^{2+}$  are very likely to be due to better complex-substrate interactions inducing much more efficient excited-state deactivation. The

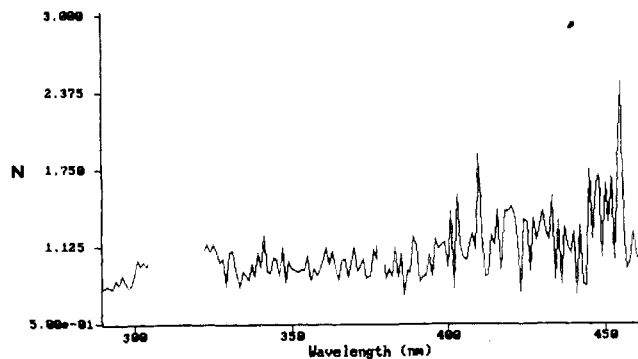


Figure 5. Polarization ratio ( $N$ ) measured along the excitation spectrum of  $Pt_3(dppm)_3CO^{2+}$  in 2-MeTHF at 77 K.

hypothesis is consistent with the fact that clear isosbestic points appear in the  $Pd_3(dppm)_3CO^{2+}$  UV-visible spectra upon addition of a different solvent to the solutions, while barely observable changes are noticed for  $Pt_3(dppm)_3CO^{2+}$  upon addition of the same substrate.

**3. Polarized Spectra.** The emission intensity of the  $Pt_3(dppm)_3CO^{2+}$  compound was great enough that the photoselection technique could be applied.<sup>14,22</sup> To obtain absorption polarizations by this method, we must know the emission polarization relative to the molecular axis. The polarization ratio,  $N$ , is given by  $(I_V/I_H)(I_H/I_V)_H$  where  $(I_V/I_H)_V$  is the ratio of the intensities of vertically to horizontally polarized emissions when excited with vertically polarized light and  $(I_H/I_V)_H$  is the ratio of the intensities of horizontal and vertical emissions with horizontally polarized excitation.  $N$  is then related to the relative orientation of transition moments in absorption and emission. The theoretical value of  $N = 3$  indicates that the absorption is polarized along a single molecular axis followed by an emission along the same axis.  $N = 0.5$  indicates single-axis absorption followed by emission along a perpendicular axis. (In practice, the theoretical values were never obtained; this is due in part to the natural depolarization of the glass.) The  $C_{3v}$  geometry of the molecule allows only two transition polarizations to occur: along the  $z$  axis and along the  $x,y$  plane. Hence an absorption polarized along the  $z$  axis followed by an emission parallelly polarized would produce a polarization ratio approaching the theoretical value of 3.0. On the other hand, one optical process involving  $x,y$ -plane polarization will generate a polarization ratio of 1.0 (depolarized light). Theoretically, only the  $a_2 \rightarrow a_2$  and  $a_1 \rightarrow a_1$  transitions should be  $z$ -polarized. There is no low-energy  $a_1 \rightarrow a_1$  transition, but a relatively medium-energy  $a_2(42) \rightarrow a_2(34)$  transition should occur (see Figure 2)

(22) See for example: Brummer, J. G.; Crosby, G. A. *Chem. Phys. Lett.* **1984**, *112*, 15.

and would be expected somewhere in the high-energy region of the spectra (i.e.  $\leq 300$  nm in Figure 1). The polarization ratios for emission excitation of  $[Pt_3(dppm)_3CO](PF_6)_2$  in a 2-MeTHF solution are shown in Figure 5. The polarization ratios are  $\sim 1$  all along the spectrum (290–460 nm), indicating that the electronic transitions are all depolarized and also indicating that the results are consistent with an  $e \rightarrow a_2$  assignment (since orbitals 36–41 have  $e$  symmetry).

The  $a_1 \rightarrow a_2$  transition cannot be optically pumped via a direct excitation.  $^3A_2$  and  $^3E$  excited states lie nearby and, including the effect of spin-orbit coupling on these states, produce  $A_1 + E$  and  $A_1 + A_2 + 2E$ , respectively. Generally the  $A_1(z)$  state is the most stable one,<sup>22</sup> and it still appears to be impossible to make an assignment whether the  $^3A_2$  or  $^3E$  excited state is the emissive one on the basis of our polarization results. Since the polarization ratios did not increase when approaching the low-energy region, we conclude that the  $a_2(42) \rightarrow a_2(34)$  transition is located below 290 nm.

In connection with the  $^3A_2$  vs  $^3E$  problem, low-temperature MCD experiments<sup>12</sup> or very low-temperature emission spectroscopy with the application of high magnetic fields or photophysical data measurements as a function of temperature (4–300 K) could be alternative methods to be employed to make any definitive assignment.

### Concluding Remarks

The nature of the frontier orbitals in the  $M_3(dppm)_3CO^{2+}$  clusters has been experimentally addressed, and our results have confirmed the EHMO findings. Even though we have not been able to assign the lowest energy triplet excited states ( $^3A_2$  vs  $^3E$ ), the excited-state chemistry should be very similar for both states. The antibonding character of the LUMO suggests that the M–M distances should be greater in the excited state, which implies that the molecular cavity can accommodate larger substrates with respect to the ground-state structure. The cluster–substrate interactions occurring within this cavity govern the excited-state deactivation processes, and one should expect the presence of photoinduced reactivities between the clusters and relatively larger substrates. This area is a topic of current research in our laboratory.

**Acknowledgment.** We thank Dr. S. Hubig (Center for Fast Kinetics) for the picosecond flash photolysis measurements. P.D.H. thanks Dr. V. M. Miskowski (Beckman Institute) for fruitful discussions. This research was supported by the NSERC (Canada), the FCAR (Québec), and the Bureau de la recherche (Université de Sherbrooke).

**Supplementary Material Available:** Tables giving UV-visible data for  $Pt_3(dppm)_3CO^{2+}$  and EHMO atomic contributions for orbitals 32–37 (5 pages). Ordering information is given on any current masthead page.